

# Lawrence Berkeley National Laboratory

## Recent Work

### Title

A LARGE-APERTURE HIGH-EFFICIENCY ION DETECTOR

### Permalink

<https://escholarship.org/uc/item/7hb49674>

### Authors

Gibbs, Hyatt M.  
Commins, Eugene D.

### Publication Date

1966-02-17

**University of California**

**Ernest O. Lawrence  
Radiation Laboratory**

A LARGE-APERTURE HIGH-EFFICIENCY ION DETECTOR

**TWO-WEEK LOAN COPY**

*This is a Library Circulating Copy  
which may be borrowed for two weeks.  
For a personal retention copy, call  
Tech. Info. Division, Ext. 5545*

**Berkeley, California**

## DISCLAIMER

This document was prepared as an account of work sponsored by the United States Government. While this document is believed to contain correct information, neither the United States Government nor any agency thereof, nor the Regents of the University of California, nor any of their employees, makes any warranty, express or implied, or assumes any legal responsibility for the accuracy, completeness, or usefulness of any information, apparatus, product, or process disclosed, or represents that its use would not infringe privately owned rights. Reference herein to any specific commercial product, process, or service by its trade name, trademark, manufacturer, or otherwise, does not necessarily constitute or imply its endorsement, recommendation, or favoring by the United States Government or any agency thereof, or the Regents of the University of California. The views and opinions of authors expressed herein do not necessarily state or reflect those of the United States Government or any agency thereof or the Regents of the University of California.

UNIVERSITY OF CALIFORNIA

Lawrence Radiation Laboratory  
Berkeley, California

AEC Contract No. W-7405-eng-48

A LARGE-APERTURE HIGH-EFFICIENCY ION DETECTOR

Hyatt M. Gibbs and Eugene D. Commins

February 17, 1966

## A LARGE-APERTURE HIGH-EFFICIENCY ION DETECTOR\*

Hyatt M. Gibbs and Eugene D. Commins†

Physics Department and Lawrence Radiation Laboratory  
University of California, Berkeley, California

February 17, 1966

## ABSTRACT

A simple, highly efficient detector has been developed for negative ions that is similar to Ridley's for positive ions. The negative ions are accelerated to 10 keV, strike a Duralumin surface at 45 deg incident angle, and eject secondary electrons. These are in turn accelerated by 10 keV and focused crudely onto a plastic scintillator joined to an RCA 8575 photomultiplier tube. The detector has an entrance aperture of 5×5 cm, over which the sensitivity is uniform. The Duralumin surface requires no special preparation other than perfunctory initial cleaning, and the detector functions with excellent stability even in a rather poor vacuum ( $\approx 10^{-5}$  torr). With appropriate voltage changes in the ion source the detector has been tested successfully for most of the positive alkali ions as well as the negative halogen ions  $F^-$ ,  $Cl^-$ ,  $Br^-$ , and  $I^-$ . The detector noise is a few counts per second at efficiencies exceeding 90% for all these ions, excluding grid losses.

## I. INTRODUCTION

The detector described here has been developed to observe negative recoil ions in several  $\beta$ -decay angular correlation experiments. These experiments require a detector of low noise, good stability, and large entrance aperture, over which the sensitivity should be high and uniform. Electrodes requiring no elaborate surface preparation--such as heat treatment, etc.--are desirable for simplicity in construction and operation. The design chosen is basically Ridley's,<sup>1</sup> with suitable modifications for negative ions.

A simple ion source and selector were constructed to test the detector, consisting of a tungsten filament coated with alkali halides and  $\text{KHF}_2$  to emit positive alkali ions and negative halogen ions upon heating,<sup>2</sup> low-voltage accelerating electrodes, a crude 90-deg mass spectrometer, and a number of defining electrodes. The investigation centered about  $\text{F}^-$ , but  $\text{Cl}^-$ ,  $\text{Br}^-$ ,  $\text{I}^-$ ,  $\text{Li}^+$ ,  $\text{Na}^+$ ,  $\text{K}^+$ , and  $\text{Rb}^+$  were also studied. The ions to be detected are accelerated to 10 keV energy and allowed to strike a Duralumin surface at 45 deg incident angle. The ion beam is of rather small cross section ( $1 \text{ cm}^2$ ) compared with the entrance aperture of the detector, and can be deflected electrostatically to strike any desired portion of the detector surface. In this way it was possible to investigate the spatial uniformity of the detector.

The secondary electrons liberated at the detector surface are accelerated through 10 keV and focused onto a plastic scintillator joined to an RCA 8575 photomultiplier tube. This arrangement, as pointed out by Ridley, combines the high-gain low-noise characteristics of a conventional electron multiplier with the excellent stability of the scintillator-photomultiplier

system. The 8575 tube was chosen for its high quantum efficiency, low dark current, and ready availability at the Lawrence Radiation Laboratory in Berkeley.

The detector efficiency was determined by comparing the detector counting rate with a direct measurement of the ion beam current. The latter is determined by a retractable collector placed directly in the ion beam and connected to a sensitive electrometer.

An overall efficiency of at least 75% was achieved for  $F^-$ , in which almost all losses are due to grid opacity. At this efficiency the detector noise is a few counts per second. The noise level is slightly higher than that achieved by Ridley, but could probably be reduced by scrupulous attention to the sources of high voltage noise (dust, etc) and by careful photomultiplier tube selection.

There was no noticeable change in the quality of the photomultiplier pulse spectrum over the duration of the tests (several months), during which the vacuum system was often open to atmosphere, and the detector surface handled many times. This is convincing evidence of the ruggedness and stability of the detector.

## II. APPARATUS

### A. Description of the Detector

Figure 1 is a cross-sectional view of the components of the detector. Both grids consist of two layers of 0.051-mm (0.002-in.)-diameter tungsten wire with a pitch of 0.635 mm (40 per inch). The brass box is smoothly polished; the entrance and exit apertures are squares with sides of 5.1 cm and 3.8 cm, respectively. The back of the box is bolted to a Lucite support in the test apparatus. The secondary emission surface is ordinary Dural

stock (#2024T) with a fair polish. A Pilot B scintillator is sealed into a brass plate with epoxy; the front face is then machined to a very smooth flat surface. A layer of aluminum about  $500 \text{ \AA}$  thick is then evaporated onto the front surface. This thickness was chosen on the basis of Young's observation that the detectable luminescence increases with thickness up to  $500 \text{ \AA}$  because of the increased reflectivity (i. e., better light collection), but decreases above  $500 \text{ \AA}$  because of energy loss in the layer with no appreciable gain in reflectivity.<sup>3</sup> An RCA 8575 photomultiplier tube completes the ion detector. Its high quantum efficiency and low-noise, high-gain characteristics are essential to the successful operation of the detector. The tube used for most of the tests was chosen at random from a group of eight "good" 8575's. Essentially the same results have been observed with other 8575 tubes from this group.

The voltage divider network suggested by RCA is used:  $0.31 \text{ M}\Omega$ ,  $0.1$ ,  $0.15$ ,  $0.1$ ,  $0.1$ ,  $\dots$ ,  $0.1$ , with  $0.1\text{-}\mu\text{F}$  capacitors across the last four dynodes. The saturation that occurs at the higher voltages does no harm in this application. The focusing electrode voltage is set at  $0.85$  to  $0.90$  of the first dynode voltage (photocathode grounded); its value is not very critical. The pulse width of the output is determined by the anode resistor and its parallel capacitance. For pulse-height analysis the pulses are amplified by the Argonne type A-61 amplifier and analyzed by a RCL Model 20611 256-channel pulse-height analyzer. Counting is accomplished by two Lawrence Radiation Laboratory counting banks, each consisting of a  $10\text{-Mc}$  discriminator 3X9923 and three  $5\text{-Mc}$  decade scalars 4X1024.<sup>4</sup>



### B. Description of Test Apparatus

In order to optimize the design and to test the detector, an ion source, selector, deflector, and calibration detector are needed (see Fig. 2). The source consists of a tungsten ribbon filament (0.0254 mm by about 2 mm, and about 2 cm long), coated (by painting on and drying a water solution) with one or more alkali halides, or  $\text{KHF}_2$ , or both. The ions emitted by the heated filament are collimated roughly by slits and accelerated by the resonance voltage of a 90-deg mass spectrometer with a 5-cm radius. For  $\text{F}^-$  this acceleration voltage is about 100 V. A field of about 1200 gauss is supplied by a CU-514 Indiana Steel Products Division permanent magnet with pole pieces designed to give a 1 cm gap. The analyzing magnet is followed by three defining electrodes with holes about 1 to 1.5 mm in diameter and 3 cm apart. The filament current required for beam currents of  $10^{-12}$  to  $10^{-11}$  A are 3 to 5 A for positive alkali ions and 6 to 10 A for negative halogen ions. Care must be taken to prevent the filament light from reaching the photomultiplier tube. The entire source-selector unit is mounted in a cage. For negative ions the cage is floated at -20 kV, requiring an isolation transformer and adequate insulation to supply the filament current. Presumably, one could place the source at ground, the detector box at +10 kV, and the scintillator at +20 kV, and still have the photocathode at ground by using a light pipe between the scintillator and phototube.

The efficiency measurements are made by comparing the counting rate with the current to the retractable collector inserted into the beam between two grounded grids separating the cage and detector regions. Keithley 600A and 610A electrometers serve to measure the small currents.

To test the uniformity of response of the detector two pairs of deflector plates in a shielding cage are attached to the source cage, allowing the beam to be deflected while it is still at low energy. The plates are about 2.5 cm long separated by 1 and 1.3 cm.

### III. DETECTOR CHARACTERISTICS

#### A. Secondary Emission Surface

The primary requirement for the detector surface is a large secondary-emission coefficient  $\gamma$  for incident ions. If a Poisson distribution of ejected electrons with mean value  $\gamma$  is assumed, then the probability that no electron will be ejected is 0.37 for  $\gamma = 1$ , 0.14 for  $\gamma = 2$ , 0.05 for  $\gamma = 3$ , 0.02 for  $\gamma = 4$ , etc. Evidently one should strive for  $\gamma \geq 4$  if possible. Aluminum was chosen as the first candidate on the basis of work by Bourne et al.<sup>5</sup> Beryllium-copper is also suggested, having been investigated by several workers. Chambers' results indicate that heat treatment of Be-Cu makes little difference in the  $\gamma$  for electron ejection by ions.<sup>6</sup> However, Ridley did oxidize his Be-Cu surface.<sup>1</sup> Chambers also demonstrated the advantage of using a small angle of incidence.<sup>6</sup> Figure 3 shows the results of our  $\gamma$  measurements for Be-Cu and Al at 90 deg and for Al at 45 deg, using  $F^-$  ions in the energy range 2.5 to 15 keV. The surfaces are prepared merely by sanding with silicon carbide paper and rinsing with acetone, as suggested by Chambers. The  $\gamma$  measurements are made with the detector surface inside the detector box but insulated from it. With the box grounded the surface is biased to  $\pm 30$  volts and the currents  $i_b$  and  $i_s - i_b$  are determined with an electrometer. Here  $i_b$  refers to beam current and  $i_s$  to secondary electron current. The secondary ejection coefficient is

$\gamma = i_s/i_b$ . Essentially the same results are found by using  $\pm 67.5$  or  $\pm 300$  volts bias, or by measuring  $i_b$  at the retractable collector rather than at the detector surface.

However, this was not the case for positive alkali ions. For example, with an ion energy of 10 keV and an incident angle of 45 deg, the method of reversal of detector surface voltage yields apparent  $\gamma$ 's of 18, 11, and 7 for  $K^+$ ,  $Na^+$ , and  $Li^+$  respectively. This clearly contradicts the estimate of  $\gamma$  furnished by comparison of the pulse-height spectra of these ions with that of  $F^-$ . It also disagrees with  $\gamma$ 's obtained by other workers. Measurements of the beam current at the retractable collector give  $\gamma$ 's of 4.7, 4.0, and 2.9 for  $K^+$ ,  $Na^+$ , and  $Li^+$ , respectively, which agree well with the pulse-height comparison with  $F^-$ . Moreover, for 90-deg incidence, measurements of  $i_b$  at the retractable electrode and at the detector surface agree, giving  $\gamma \approx 4.1$  for  $K^+$  at 10 keV. The discrepancy in the detector surface measurement for positive alkali ions at 45 deg is believed to arise from the unusually large reflection coefficient for these ions.<sup>7</sup> They apparently leave the surface only after most of their energy has been expended in ejecting secondary electrons.

#### B. Focusing the Secondaries on the Scintillator

To investigate the focusing properties (in two dimensions) of various box designs, rubber sheet models were constructed.<sup>8</sup> It was first feared that the secondary extraction field between the scintillator and box might also cause negative ions to miss the detector surface. The rubber sheet model indicated that the field penetrating the box is small, and later measurements showed that if the box potential is 500 volts higher than that of the detector surface, very few secondaries are extracted by the 10 kV box-to-

scintillator voltage. The primary ions have such high energy (10 keV) that they move in practically straight lines through the detector box. The other predictions from the study of the rubber sheet model were verified by observing visually the luminescent scintillator spot (about 0.5 cm in diameter) arising from the secondaries ejected by an intense  $F^-$  beam. With the detector configuration of Fig. 1 and with the beam centered, the position of the spot relative to the scintillator is centered vertically and slightly to the right of center (looking from outside the chamber). Upward (or right) displacements of the beam result in downward (or left) displacements of the spot. Practically all of the 2.5-cm-diameter scintillator surface is used. The focusing is crude, but adequate.

### C. Output Pulse Shape and Distribution

A typical output from the photomultiplier is represented in Fig. 4. The large-amplitude pulses are the  $F^-$  signal, and the smaller are noise and after-pulses (see III. D.). Lengthening these pulses to about 1  $\mu$ sec permits pulse-height analysis with the RCL analyzer, as in Fig. 5 (also Figs. 7 and 8).

### D. Efficiency

Figure 5 demonstrates the good separation between the signal and noise. Several efficiency checks were made as follows. A pulse-height curve is mapped out by taking differences with the 10-Mc discriminator. The discriminator is set to exclude the high-intensity low-height noise pulses, i. e., it is set just to the right of the sharp break in Fig. 5. The true signal above that pulse height is obtained by subtracting the counting rates with and without an accelerating resonance voltage for the ions in the source. The true ion current is measured with the retractable collector at +30 volts (the same results were obtained with 67.5 or 300 volts) and an

electrometer. A typical measurement yielded 78% for the overall efficiency. The expected efficiency for 85% calculated grid transmission (assuming each double grid appears single) was 81%, including a correction for the discriminator dead time. (Counting rates of about  $10^5$  per second were employed to minimize dead-time corrections.) The resulting efficiency of 96 or 97% (excluding grid losses) at a reasonable noise level is in good agreement with a direct analysis of the pulse-height distributions. Of course, the grid transmission can be increased to 95% or so, to increase the overall efficiency.

Pulses with amplitude below the discriminator threshold and proportional in number to the signal counting rate were also observed. It was finally shown with a barium titanate flash lamp that this effect is produced by afterpulses arising from some feedback mechanism in the photomultiplier.<sup>9</sup> Fortunately, the signal and afterpulses are well separated in amplitude.

#### E. Uniformity

The spatial uniformity of the detector efficiency was investigated by electrostatic deflection of the ion beam. The results are shown in Fig. 6. In each scan the wires of the grid at the exit of the deflector cage were parallel to the direction of deflection. Scans taken perpendicular to the wires showed 5 to 10% variations, presumably arising from the change in transmission characteristics of the double grid with a change in the angle of incidence of the slow ions.

The deflector plates were calibrated by observing the ion current to a 5-cm-square collector inside the box. The results of Fig. 6 show that the detector is sensitive over the full  $5 \times 5$ -cm aperture. The gradual dropoff at the edges of the scans is a result of the finite size of the beam

( $\approx 1$  cm diameter). There is no deterioration of the pulse distribution as the beam is scanned past the edge and the intensity drops to zero.

#### F. Magnetic Field Shielding

The RCA 8575 efficiency can be reduced 50% by a magnetic field of less than 1 gauss. Consequently, the ion signal is destroyed by a small field if no shield is used. With a photomultiplier mu-metal shield, no change in pulse distribution is observed when a field of 2 gauss is applied to the box and photomultiplier in any direction. Higher fields were not tried. Because the focusing of the secondaries is so crude, it is not surprising that the detector is unaffected by small magnetic fields.

#### G. Noise

Most of the detector measurements were made with a photomultiplier voltage of 2.9 kV, for which the signal output pulses were fed into the 10-Mc discriminator without further amplification. With the discriminator set to separate the signal and noise as described in Section III. D, the noise is 40 to 50 counts per second. Because the detector was designed for coincidence measurements, this noise rate is acceptable. Consequently, no extensive efforts to reduce the noise were made.

Since others may be interested in using this detector in noncoincidence experiments, further comments on the noise may be appropriate. With reasonable care to eliminate noise arising from the high voltages applied to the detector box and source, the principal source of noise is the photomultiplier. This noise drops considerably with a decrease in photomultiplier voltage, and noise rates of only a few per second have been found at 2 kV with the discriminator set to accept more than 95% of the signal (excluding grid losses). With a discriminator acceptance of 50% of

the signal, the noise rate is less than 1 count per second. For example, compare Figs. 5 and 7a, which were taken with approximately the same ion beam intensity but different photomultiplier voltages. The noise in the 8575 tube has two components: (a) the usual photocathode and dynode noise, which yields a pulse distribution dropping off rapidly in the few-photoelectron region; and (b) a much smaller component, which drops off many times more slowly and extends into the many-photoelectron region.<sup>10</sup> The second component is the annoying factor in the present application. Perhaps another tube would have a smaller second component than the 8575, even though the total noise current might be higher.

#### H. Response to Other Ions

The ease with which positive alkali ions and negative halogen ions are obtained from the simple source makes it easy to calibrate the mass spectrometer and investigate the response of the  $F^-$  detector to other ions. The results are presented in Figs. 7 and 8. The efficiency decreases with increased halogen mass, but increases with increased alkali mass. (The latter effect might arise from alkali ion reflection, which is larger for the lighter alkalis. Perhaps Ridley's method of 90 deg incidence on activated Be-Cu is preferable for positive alkali ions.) For all the ions investigated the signal and noise are well resolved. This can be improved by applying higher accelerating potentials, as shown in Fig. 8 for  $K^+$ , but this must be accompanied by increased care to eliminate high-voltage noise.

#### IV. ACKNOWLEDGMENTS

We are grateful to Frank P. Calaprice for a number of very useful discussions.

We wish to thank Professor Leonard Loeb's group, particularly William Winn and Paul Burrow, for extended use of their electrometers, and Professor Howard Shugart for use of the pulse-height analyzer.



FOOTNOTES AND REFERENCES

\* Work supported by the U. S. Atomic Energy Commission.

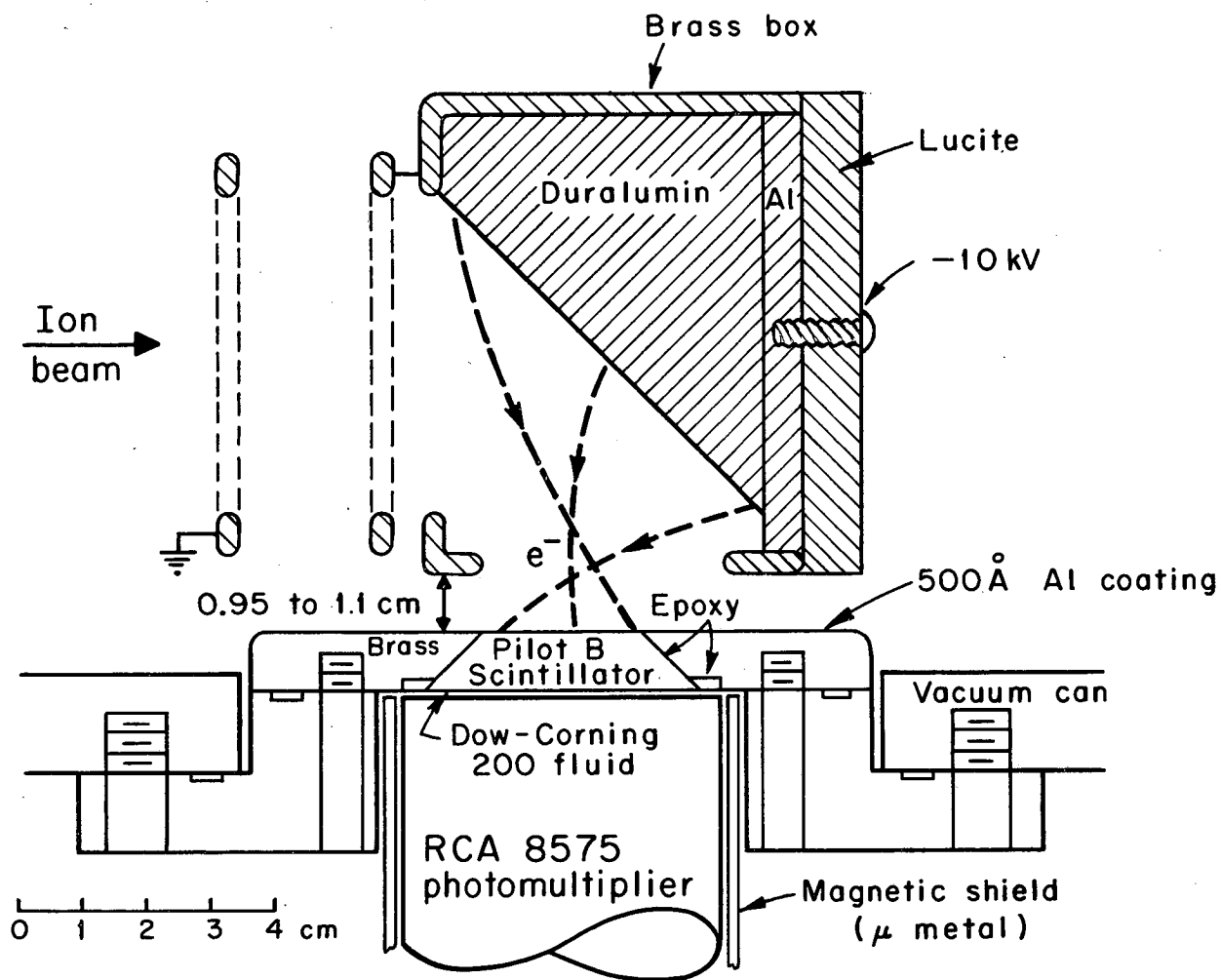
† Alfred P. Sloan Fellow

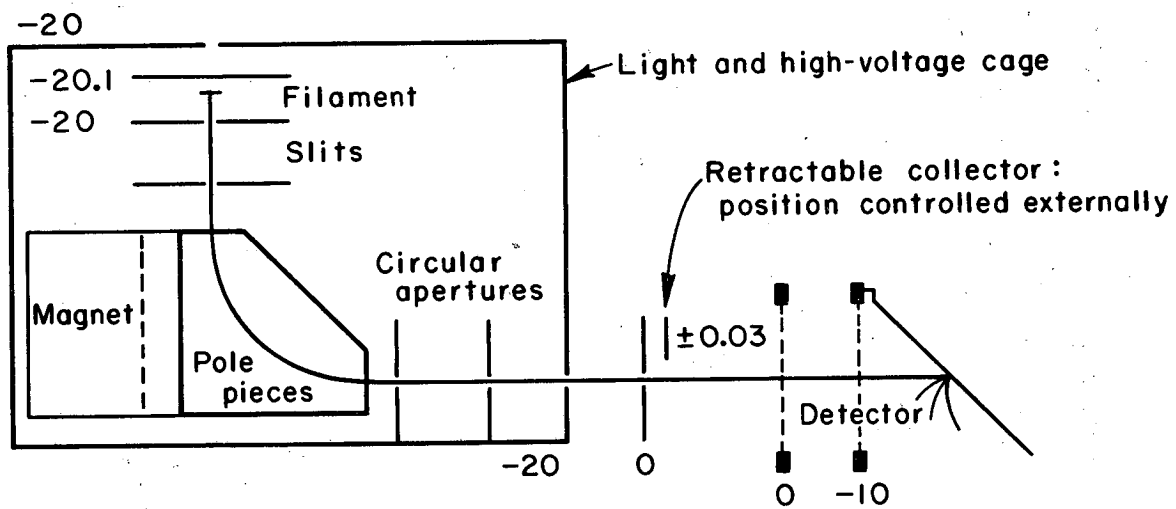
1. B. W. Ridley, *Nucl. Instr. Methods* 14, 231 (1961).
2. E. Ya. Zandberg and N. I. Ionov, *Soviet Physics - Uspekhi* 67 (2), 255 (1959); M. Kaminsky, Atomic and Ionic Impact Phenomena on Metal Surfaces (Academic Press, Inc., New York, 1965), pp. 110-141.
3. J. R. Young, *J. Appl. Phys.* 27, 1 (1956).
4. See the Lawrence Radiation Laboratory Counting Handbook, edited by the Nuclear Instrumentation Groups, Lawrence Radiation Laboratory Report UCRL-3307, June 1964.
5. H. C. Bourne, Jr., R. W. Cloud, and J. G. Trump, *J. Appl. Phys.* 26, 596 (1955).
6. E. S. Chambers, *Phys. Rev.* 133, A1202 (1964).
7. C. Brunnée, *Z. Physik* 147, 161 (1957). See also M. Kaminsky, Atomic and Ionic Impact Phenomena on Metal Surfaces (Academic Press, Inc., New York, 1965).
8. J. R. Pierce, Theory and Design of Electron Beams (D. Van Nostrand Co., Inc., New York, 1954), Chapter V.
9. RCA Phototubes and Photocells, RCA Technical Manual PT-60, C1963, pp. 60-61.
10. K. Siegbahn, Alpha-, Beta- and Gamma-Ray Spectroscopy (North-Holland Publishing Co., Amsterdam, 1965), p. 280; H. R. Krall, *IEEE Trans. Nucl. Sci.* NS-12, 39 (1965).

## FIGURE CAPTIONS

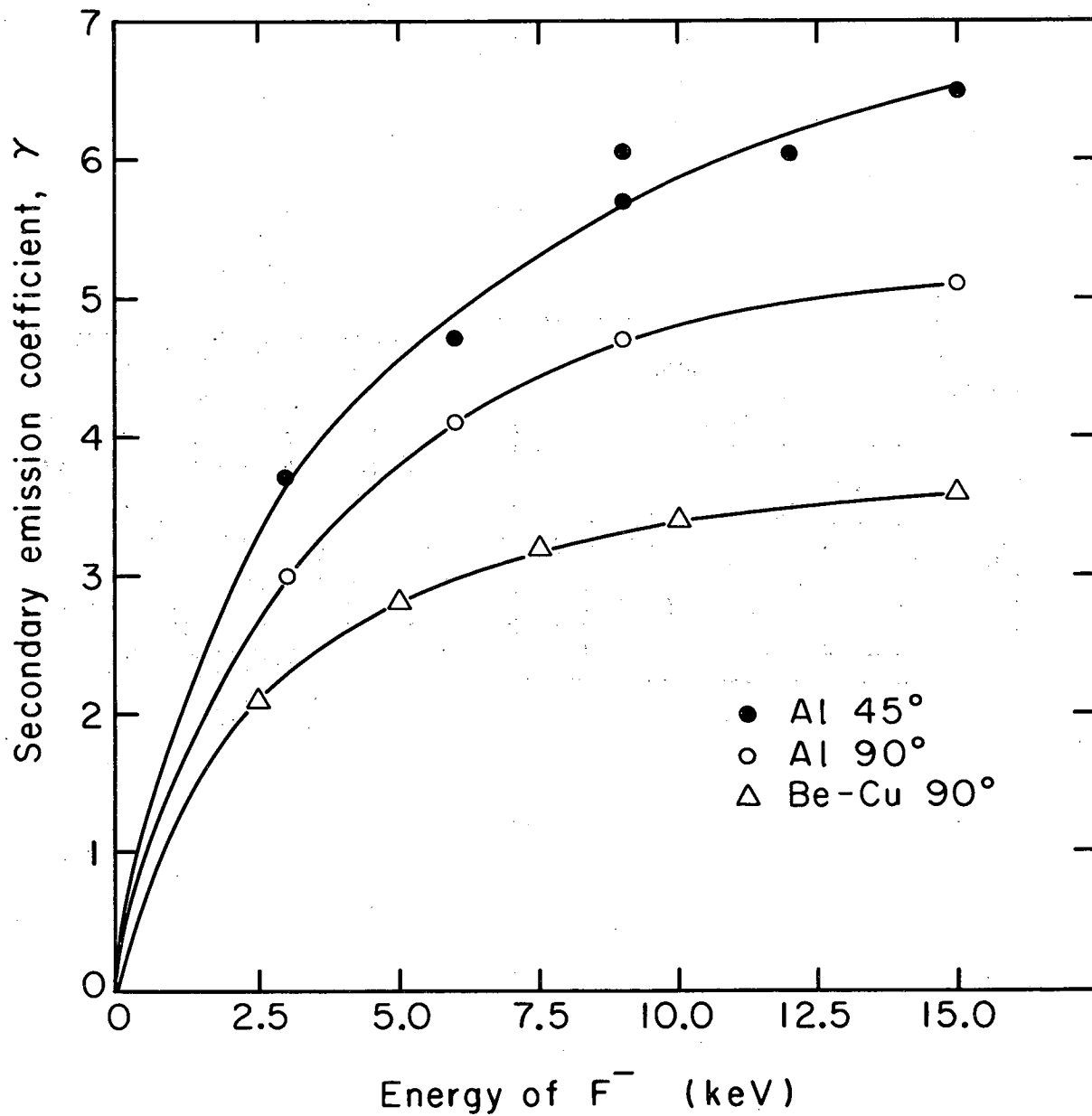
- Fig. 1. Cross-sectional view of ion detector.
- Fig. 2. Schematic diagram of test apparatus. Numbers are voltages in kilovolts.
- Fig. 3. Secondary emission coefficients of  $F^-$  ions on Be-Cu and Al as a function of energy.
- Fig. 4. Photomultiplier output observed with a Tektronix 585 oscilloscope: 1 volt/cm, 10 nsec/cm;  $F^-$  source voltage -20 kV, detector box -10 kV, and photomultiplier 2.9 kV.
- Fig. 5. Pulse amplitude distribution as found with a RCL pulse-height analyzer: 1023 counts per channel full scale, 2 min accumulation time,  $F^-$  source voltage -20 kV, detector box -10 kV, and photomultiplier 1.9 kV. Lower trace shows noise with accelerating resonance voltage off.
- Fig. 6. Uniformity of response of detector to vertical and horizontal deflections of the incident  $F^-$  beam:  $F^-$  source voltage -20 kV, detector box -10 kV, and photomultiplier 2.9 kV. V and H refer to vertical and horizontal deflector voltages. The discriminator is set to eliminate most of the noise pulses. Considering the crudeness of the deflector system, these uniformity scans give no indication that the detector is not perfectly uniform.
- Fig. 7. Pulse-height distributions showing the response of the detector to various negative ions. Source -20 kV, box -10 kV, photomultiplier 2.9 kV, 2 min accumulation, 2047 display scale, 65% live time. (a)  $F^-$ ; (b)  $Cl^-$ ; (c)  $Br^-$ ; (d)  $I^-$ ; (e) unknown around mass 200. Similar curve was obtained for another unknown of mass 26 thought to be  $CN^-$ .

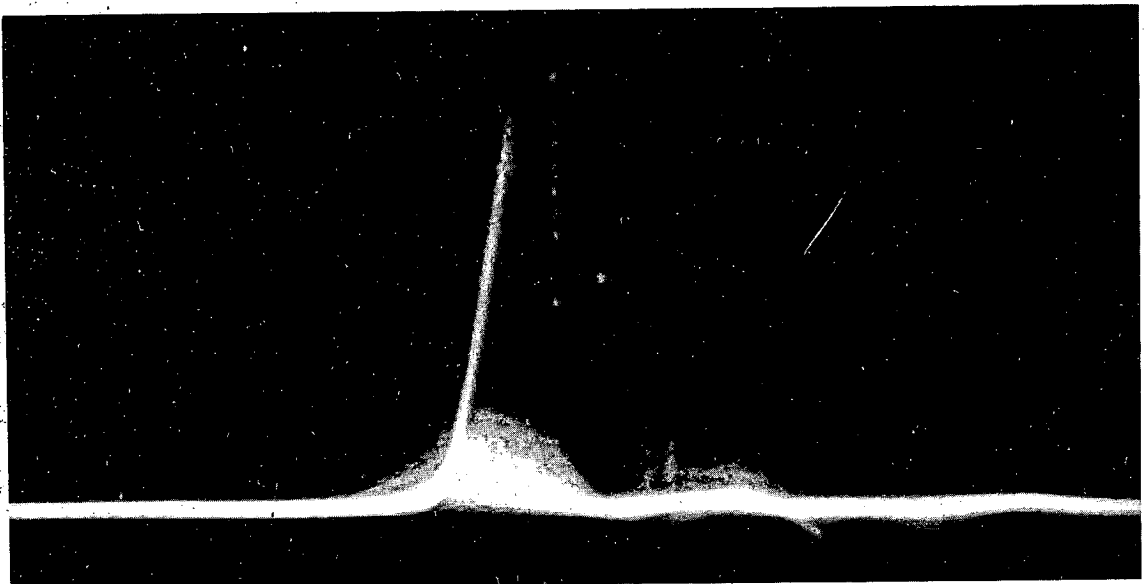
Fig. 8. Pulse height-distributions showing the response of the detector to various positive ions. Source at ground, box -12.5 kV (except where noted otherwise), other conditions as in Fig. 8, (a)  ${}^6\text{Li}^+$ ; (b)  ${}^7\text{Li}^+$ ; (c)  $\text{Na}^+$ ; (d)  $\text{K}^+$ , box -10 kV; (e)  $\text{K}^+$ , box -12.5 kV; (f)  $\text{K}^+$ , box -15 kV; (g) unknown, mass about 56; (h)  $\text{Rb}^+$ .



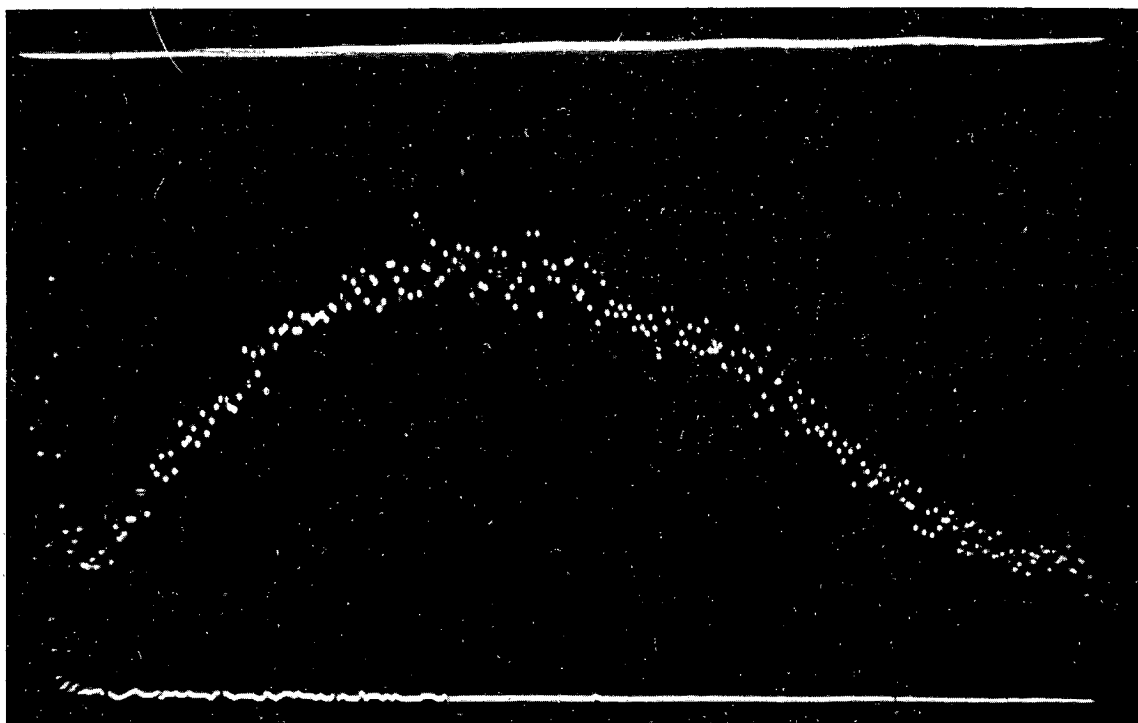


MUB-9682





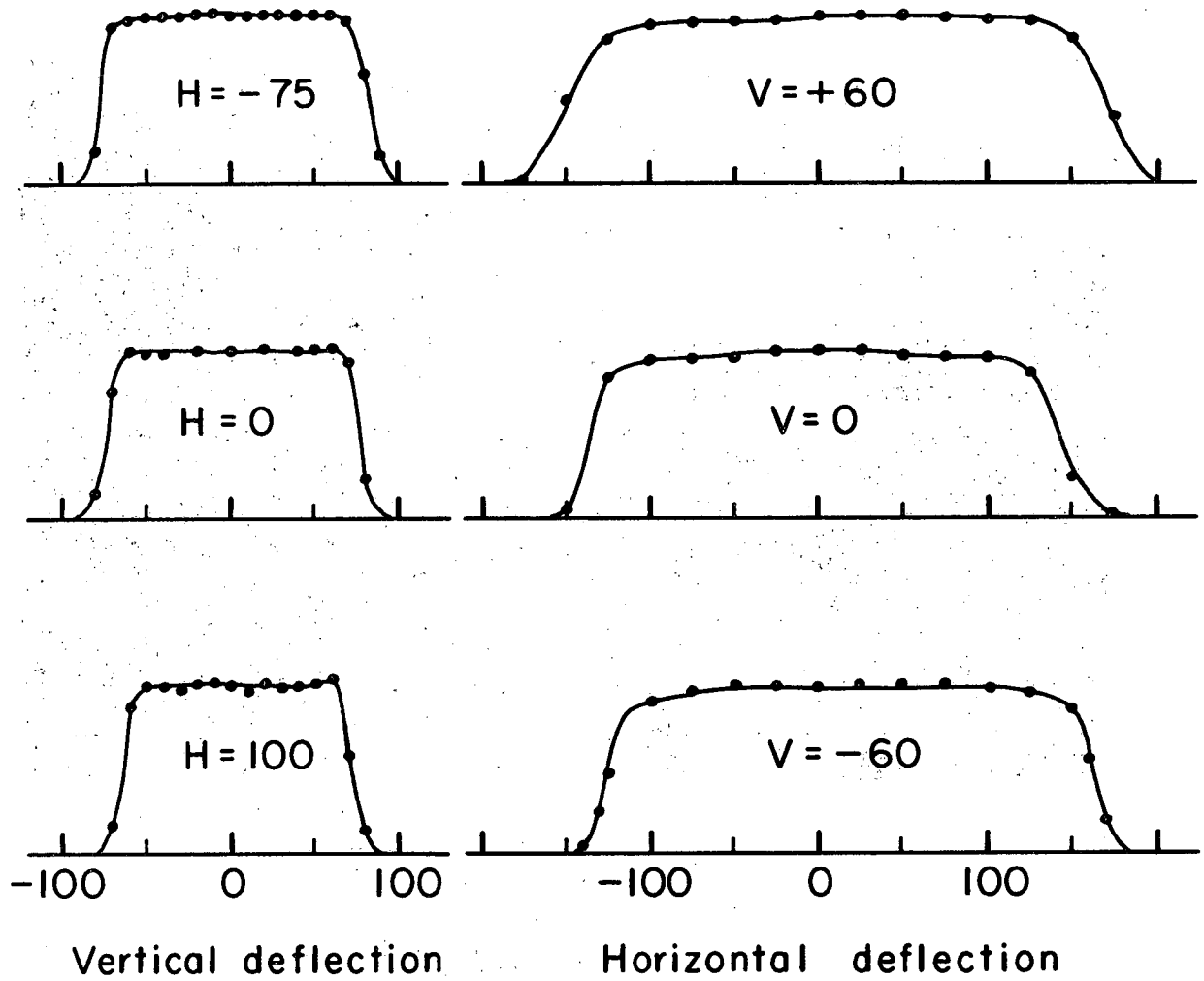
ZN-5420

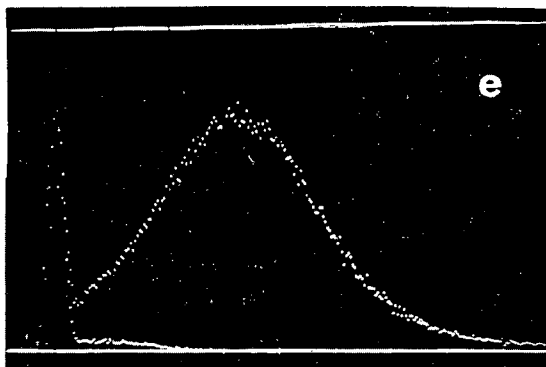
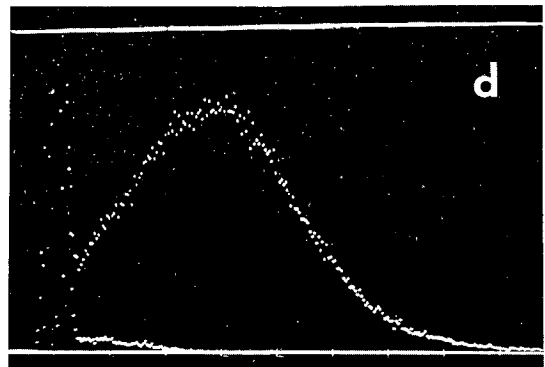
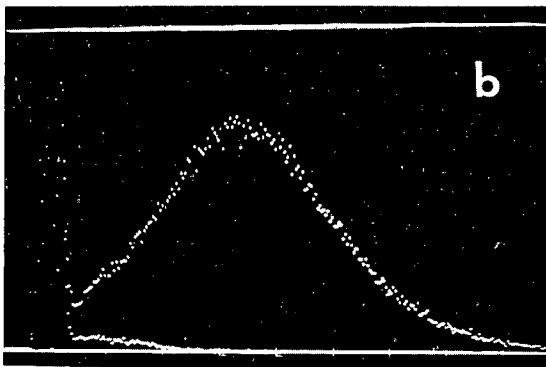
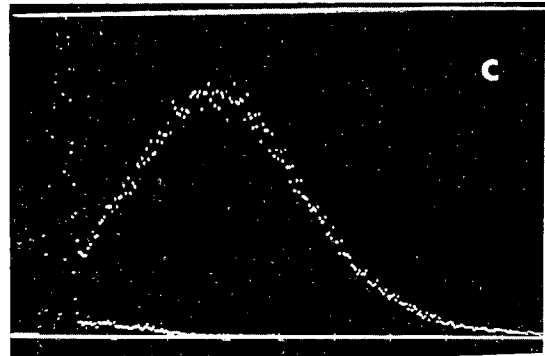
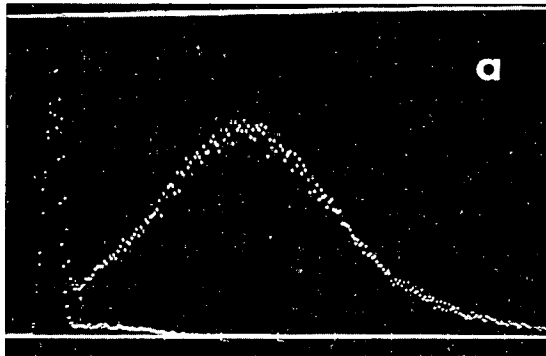


ZN-5421

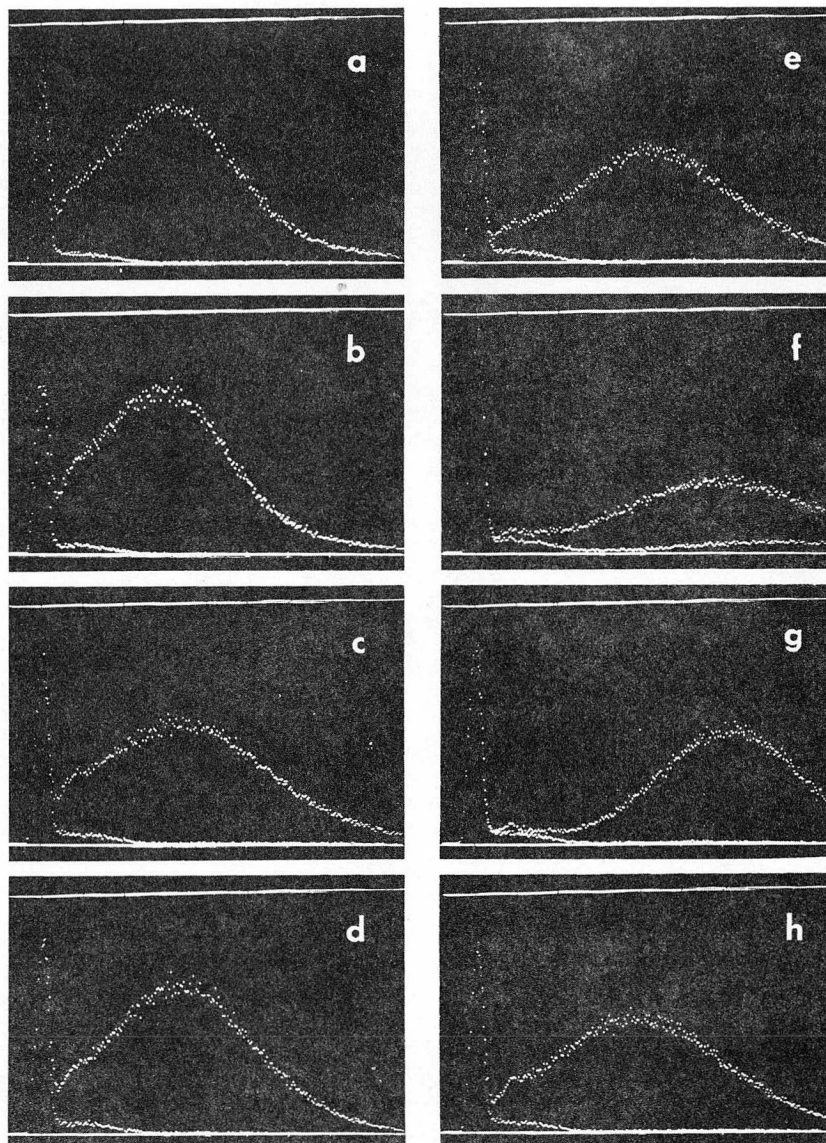
r  
e  
x  
t







ZN-5422



ZN-5423

This report was prepared as an account of Government sponsored work. Neither the United States, nor the Commission, nor any person acting on behalf of the Commission:

- A. Makes any warranty or representation, expressed or implied, with respect to the accuracy, completeness, or usefulness of the information contained in this report, or that the use of any information, apparatus, method, or process disclosed in this report may not infringe privately owned rights; or
- B. Assumes any liabilities with respect to the use of, or for damages resulting from the use of any information, apparatus, method, or process disclosed in this report.

As used in the above, "person acting on behalf of the Commission" includes any employee or contractor of the Commission, or employee of such contractor, to the extent that such employee or contractor of the Commission, or employee of such contractor prepares, disseminates, or provides access to, any information pursuant to his employment or contract with the Commission, or his employment with such contractor.

